Numerical modeling of hydro-mechanical fracture behavior

C. Guiducci
Scuola Normale Superiore di Pisa – Italia (Italy)

A. Pellegrino
Eni - Agip Division - Italia (Italy)

J.P. Radu, F. Collin, R. Charlier
Département GéomaC – Université de Liège – Belgique (Belgium)

ABSTRACT: A numerical approach for modeling coupled hydro-mechanical fracture behavior is proposed. The movement of fluids through rock fractures is important in many engineering areas of practical interest such as those ones of petroleum and mining engineering. In that context, one of the most investigated and complex subjects is the effect on well productivity due to changes in hydraulic conductivity both on the matrix rock and on its main fractures. It is well known, that these flow characteristics are strongly controlled by fracture apertures. Recent investigations on the distribution of the apertures in natural fractures suggest that the cubic law can, better than the Darcy law, predict the fluid flux through rough walled fractures as long as the appropriate average fracture aperture is used. A finite element code is developed to predict the influence that the stresses variation in the soil has on the distributed hydraulic conductivity field. The proposed model combines the stochastic cubic law with a non-linear deformation function (hyperbolic) that is suggested to describe the stress-closure/opening curves of the joints and that allows to couple together the hydraulic and the mechanic fracture behavior. The relationships used and the validity of the present model are tested through comparison between experimental data and numerical predictions (Bart 2000) in various boundary and loading conditions. Comparison between the Darcy model governing fluid flow equation and linear stress-closure/opening relation has also been performed showing the differences and the better de-scription given by the proposed new model.

1 INTRODUCTION

The present paper lies its aim in the oil reservoir problems staying at the boundary between geomechanics and numerical methods. Moving from the observation that lots of the last exploited hydrocarbon reservoirs are naturally fractured, oil companies are becoming more aware that the behavior of fractured reservoirs is dependent on the good description of its hydro-mechanical behavior during the injection/production rate.

The description of a single fracture hydraulic and mechanical behavior is a subject of central importance in petroleum engineering applications. This is the basic building block of realistic models reproducing fractures system behavior and it's the subject of the present paper.

As we know, during the last years the main characteristics of the behavior of rock fractures have been studied by analyzing the experimental investigations of many authors like Barton (1976), Bandis & al (1981). A large amount of fracture modeling work is available in the literature. Goodman & al (1968; 1972), Plesha (1995), Barton & al (1985) and Bart (2000) are some of the numerous investigators who have derived the basic equations describing fracture behavior. Their numerical investigations have been the basis of our research, which have led to the conception of the proposed model.

A constitutive model is presented in the paper to simulate the coupled behavior of fractures. The main purpose is to be able to offer, through the description of fractures and of fracture interactions with rock matrix, a good representation of fractured oil reservoir during the injection/production rate.

The numerical model presented reproduces a non-linear coupled fracture behavior when normal effective stresses are applied. The coupling is realized combining the cubic law, used to describe the fluid flow into the fracture, with a non-linear deformation function (hyperbolic) suggested to describe the stress-closure/opening curves of the fractures. Also the coupling behavior under tangential effective stresses is taken into account through the simple Mohr/Coulomb linear relation.

The proposed constitutive model was introduced as interface contact element behavior model in a finite element code.

To synthesize the work done, the present paper is mainly divided into six parts dealing with: 1) the

theoretical aspects of the model; 2) the numerical aspects of the finite element LAGAMINE code with particularly attention to the contact element; 3) an academic application of the model describing a simple geometry oil reservoir; 4) comparison of the results from the improved model and a not coupled fracture model; 5) sensitivity studies; 6) conclusions.

2 INTERFACE CONSTITUTIVE MODEL

2.1 *Mechanical law*

A particular constitutive law was introduced in the finite element LAGAMINE code to describe the links between the contact stress rate and the contact strain rate of the interface element.

This relation, deduced by Goodman's experiments, showed that the fracture closure ΔVj changes, under increasing normal stress (σ_n), in a non-linear way closing resembling a hyperbola. A characteristic example is illustrated in Figure 1. The non-linearity in the σ_n-ΔVj relation was also recognized by other authors.

From a physical point of view this behavior can be explained with the progressive mobilization of the fracture asperities. At the beginning of the test, few points are in contact and the deformations related to small normal stress are important. With the progressive fracture closure the increasing augmentation of contact between asperities lets the relative displacements becoming smaller, until an asymptotic fracture closure value is reached for very high values of applied stress.

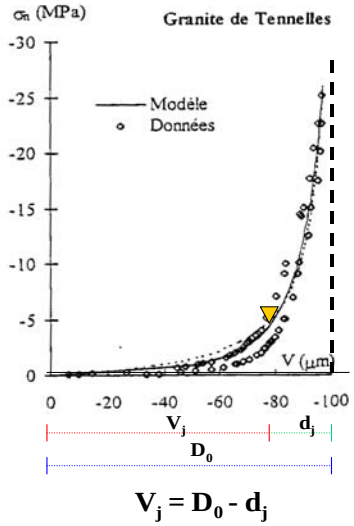

Figure 1. Normal stress-deformation relations of fractured rock.

In this paper the non-linearity in the σ_n-ΔVj relation is taken into account through the empirical hyperbolic function proposed by Bart (2000) (Fig. 1):

$$\Delta\sigma_n' = \frac{K_{ni} D_0}{\left(1+\frac{\Delta V_j}{D_0}\right)^{\gamma}} \Delta V_j \qquad (1)$$

where:

- K_{ni} is the normal initial stiffness of the fracture;
- D_0 is the asymptotical fracture opening, related to the fracture when stresses equal to zero are applied;
- γ is an empirical coefficient variable between 2 and 6, it's value is increasing with the fracture roughness. Bandis et al. (1983) proposed a value 2 to give a correct description of the mechanical behavior of the fracture.

The K_{ni} parameter can be obtained as the initial slope of the hyperbola of figure 1; its value can be estimated from the rock matrix damaged stiffness.

2.2 *Flow laws*

In this paper, water flows through the interface element is described in an anisotropic way. So, according to the definition of a transverse transmissivity T_t, two transverse fluid flows f_{t1} and f_{t2} can be described from the following relations:

$$f_{t1} = T_t\left(p_f^F - p_f^I\right) \text{ and } f_{t2} = T_t\left(p_f^I - p_f^S\right) \qquad (2)$$

where p_f^F, p_f^S and p_f^I are respectively the pressures on the two sides of the rock interface and the pressure inside the interface (at a mid position between its boundaries) (see fig. 4).

If the interface longitudinal permeability k_l is not nil, the longitudinal fluid mass flow f_l is assumed analogous to laminar flow between two perfectly smooth parallel plates. This leads to the so-called "cubic law" (Tsang and Witherspoon, 1981):

$$f_l = -\frac{d^3}{12\mu_f}\left(\underline{\nabla} p_f + \rho_f g \underline{\nabla} z\right)\rho_f \qquad (3)$$

where the volume flow rate f_l varies as the cube of separation d between the two plates; μ_f is the fluid viscosity; ∇p_f is the fluid pressure gradient along the fracture and ρ_f is the fluid density. In this case the hydraulic conductivity of a fracture with aperture d is given by:

$$k_l = d^2 \rho_f g / 12\mu_f \qquad (4)$$

3 INTERFACE FINITE ELEMENT

3.1 *General concept of a contact problem*

Consider two deformable solids (or domains) Ω^U and Ω^D with boundaries $\partial\Omega^U$ and $\partial\Omega^D$ (Fig. 2). They are contacting through boundaries $\partial\Omega^U{}_C$ and $\partial\Omega^D{}_C$.

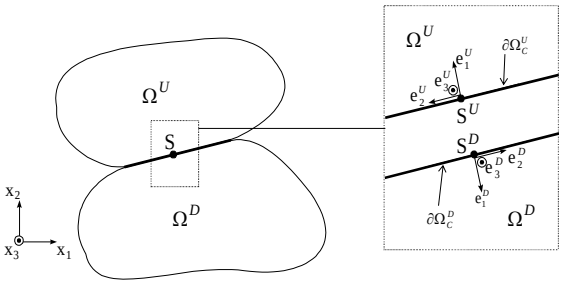

Figure 2. Contact between 2 deformable solids.

At any point *S* of the contact surface, a local triad ($\underline{e}_1$,$\underline{e}_2$,$\underline{e}_3$) can be defined for each solid as in figure 2. The $\underline{e}_1$ axis is normal to the contact whereas the $\underline{e}_2$ and $\underline{e}_3$ axes are tangent. In this local referential, for a plane or axisymmetrical problem, the stress tensor in each solid reduces to a contact stress vector $\underline{\sigma}_C$ defined by two components:

$$\underline{\sigma}_C = \begin{bmatrix} \sigma_1 \\ \sigma_2 \end{bmatrix} = \begin{bmatrix} -p \\ \tau \end{bmatrix} \tag{5}$$

with p pressure and τ shear stress. As this stress vector is defined in a local referential attached to a solid, it is independent of rigid body rotation, i.e. objective (Charlier & Cescotto, 1988). Perfectly sticking contact condition is enforced numerically using the classical penalty method which allows a small relative velocity between points S^U and S^D, i.e. a small penetration of the two solids and a relative sliding between them.

The contact stress vector $\underline{\sigma}_C$ is associated with the relative displacement velocity $\underline{\varepsilon}_c$ defined as the time derivative of the distance vector $\underline{u}$ between $\partial\Omega^U{}_C$ and $\partial\Omega^D{}_C$ (Fig. 3):

$$\dot{\underline{\varepsilon}}_C = \frac{d\underline{u}}{dt} = \underline{R}\left(\frac{d\underline{x}^D - d\underline{x}^U}{dt}\right) + \frac{d\underline{R}}{dt}\left(\underline{x}^D - \underline{x}^U\right) \tag{6}$$

where the objective distance vector $\underline{u}$ is given by:

$$\underline{u} = \underline{R}\left(\underline{x}^D - \underline{x}^U\right) \tag{7}$$

and where $\underline{R}$ represents the rotation matrix (Charlier & Cescotto 1988) between the triad ($\underline{x}_1$,$\underline{x}_2$,$\underline{x}_3$) and ($\underline{e}_1$,$\underline{e}_2$,$\underline{e}_3$). Note that through the second term of equation (6), the relative velocity of the surfaces is function of the rotation rate of the local triad, which preserves objectivity.

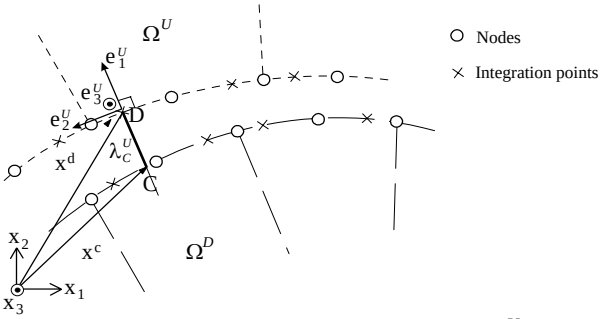

Figure 3. Parabolic interface finite elements (λ^U<0, i.e. no contact).

The contact side of each body Ω^U and Ω^D is discretised with interface isoparametric elements that are compatible with the solid finite elements discretising the corresponding body (Fig. 3). The frictional interface elements are based on mixed variational (Cescotto & Charlier, 1993): contact stresses are computed at contact element integration points whereas displacements of the solid boundary are computed at nodal points. This formulation leads to a smoother contact condition then the one based on nodal contact conditions.

The contact condition is simply obtained locally from geometrical computation of the distance λ_C between the two contact interfaces $\partial\Omega^U{}_C$ and $\partial\Omega^D{}_C$ with $\lambda_C = \underline{u}.\underline{e}_1$: - λ_C <0 no contact (Fig. 3); - $\lambda_C \geq 0$ there is contact. For more details see (Habraken & Cescotto, 1996).

3.2 *Description of the interface element*

A 2D large strain finite element has been implemented in the LAGAMINE code. It is an isoparametric element (Fig. 4), with 2 (linear) or 3 (parabolic) nodes describing the interface element side, with 3 degrees of freedom (d.o.f) per node (2 mechanical displacements *u v*, and p_f^S fluid pressure on structure side). To describe the seepage flow inside the interface, 2 or 3 further nodes are added with only 1 d.o.f. per node, the fluid pressure p_f^I inside the interface; these nodes are thus the same coordinates that the corresponding nodes on the interface element. Of course, the foundation side is defined by 2 or 3 nodes, with also 3 d.o.f per node (*u*, *v*, p_f^F fluid pressure on foundation side).

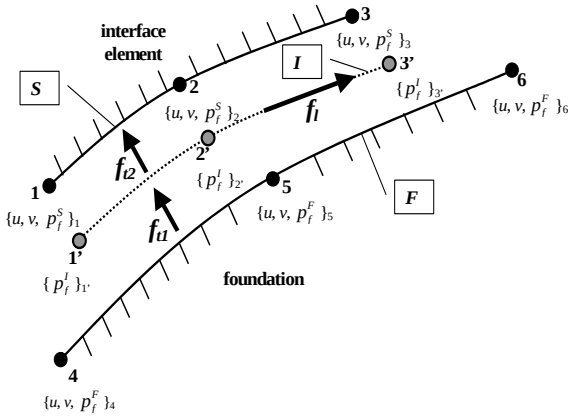

Figure 4. Description of a 2-D parabolic interface element.

With that element formulation, the equivalent nodal forces and the stiffness matrix in the Newton-Raphson sense will have, for a parabolic element, the following forms respectively given in (8) and (9):

$$\underline{F}^T = \left(\left\langle \underline{F}_S \right\rangle_{1x9} \quad \left\langle \underline{F}_I \right\rangle_{1x3} \quad \left\langle \underline{F}_F \right\rangle_{1x9}\right)^T \tag{8}$$

$$\underline{\underline{K}} = \begin{bmatrix} [\underline{\underline{K}}_{SS}]_{9x9} & [\underline{\underline{K}}_{SI}]_{9x3} & [\underline{\underline{K}}_{SF}]_{9x9} \\ [\underline{\underline{K}}_{IS}]_{3x9} & [\underline{\underline{K}}_{II}]_{3x3} & [\underline{\underline{K}}_{IF}]_{3x9} \\ [\underline{\underline{K}}_{FS}]_{9x9} & [\underline{\underline{K}}_{FI}]_{9x3} & [\underline{\underline{K}}_{FF}]_{9x9} \end{bmatrix} \quad (9)$$

where the indexes *S*, *I* and *F* respectively refer to the solid side, the interior interface and the foundation side.

4 APPLICATION

4.1 *Boundary and initial conditions*

Using the presented interface element some applications were developed. In particular, a fluid depletion of a reservoir interested by a horizontal fracture is modeled. The well is situated on the left boundary of the reservoir. For simplicity the fluid in the reservoir is considered to be water and the rock matrix is chalk. The reservoir is modeled in plane strain conditions the dimension being 2500 m of length by 300 m of height. The initial fracture opening value is ≈0.2 mm (Fig. 5).

The initial stress field is obtained, neglecting gravity effects, applying 62 MPa overburden load and a 62 MPa horizontal stress imposed on the well boundary. Initial fluid pressure of the reservoir is 48.7 MPa (Fig. 6).

A production phase was modeled starting from those initial conditions. A first step of 15 MPa fluid pressure decrease is applied for 7.5 years at the well boundary. A following second step lasting 12.5 years is perceived keeping fluid pressure constant.

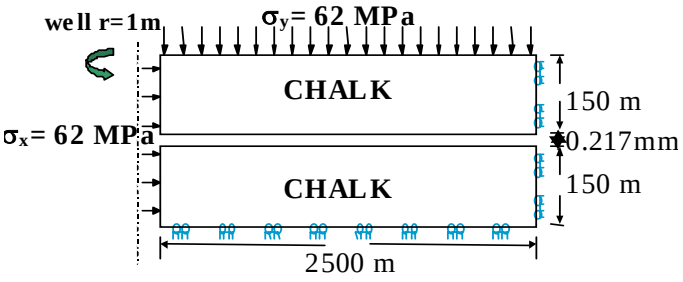

Figure 5. Mechanical boundary conditions.

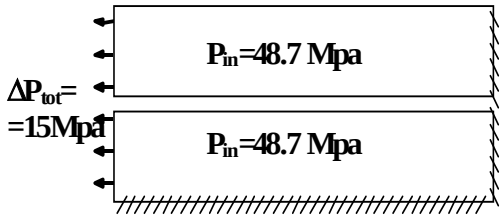

Figure 6. Hydraulic boundary conditions.

4.2 *Results*

Results regarding fluid pressure and fluid flow variation along the fracture are presented in the Figures 7-8. The curves are related to the pressure and flow evolution after 7.5 and 20 years of simulation.

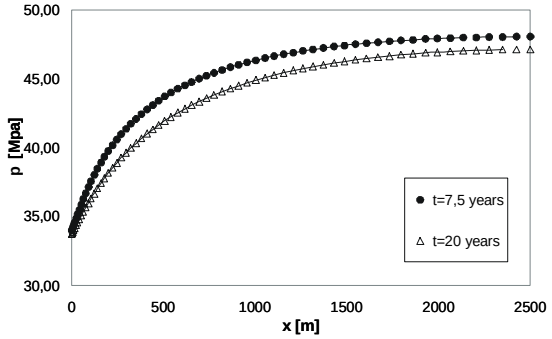

Figure 7. Fluid pressure along the fracture after 7.5 and 20 years of simulation.

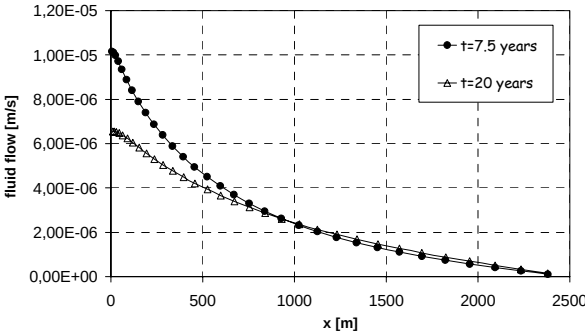

Figure 8. Fluid flow trend along the fracture after 7.5 and 20 years of simulation.

The important hydraulic role of the fracture is underlined through the flow rate evolution results (Fig. 9). The biggest flow rate outgoing from the well boundary is due to the fracture contribution. After 7.5 years of depletion a fracture flow rate maximum is reached while after, keeping pressure constant for the following 12.5 years of simulation, a small decrease is observed.

It is also observed (Fig. 9) that the contributions related to the average of the flow rate outgoing from the two rock matrix to the well are coincident and negligible compared to the flow rate associated to the fracture.

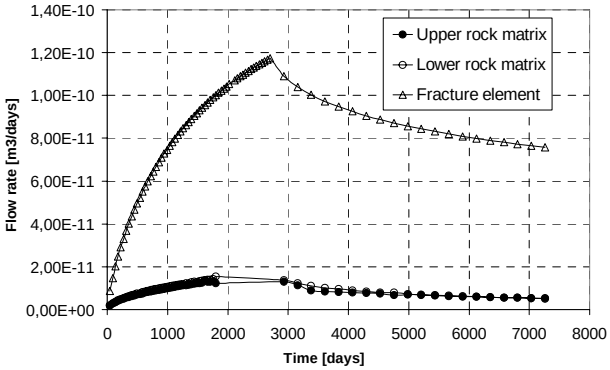

Figure 9. Outgoing flow rate variation with time increasing.

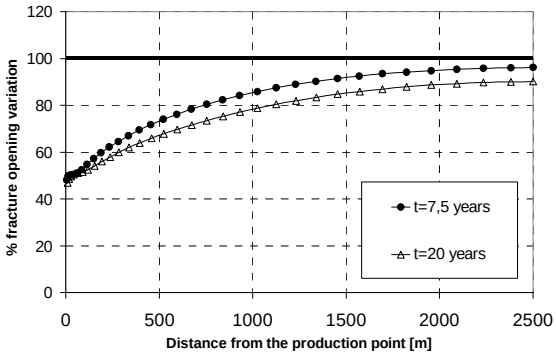

Figure 10. Fracture opening variation after 7.5 and 20 years of simulation.

Fracture coupled behavior is then put in evidence from the following results. Due to the observed fracture fluid pressure decrease, progressive fracture closure is achieved during the calculation. After 7.5 and 20 years of production simulation, Figure 10 shows that in the well nearby zone a 50% reduction of the initial fracture opening is achieved, the perturbation fading with the distance from the well is in agree with pressure variation trend.

As shown in Figure 10, the model succeeds in the representation of fracture hydro-mechanical behavior bounding pressure variation to fracture deformation. The importance of a good fracture description is underlined by comparisons between the presented fracture coupled model and a non-coupled fracture model where opening fracture is maintained constant during all the simulation time.

4.3 *Comparisons*

Two different fracture models were applied for the description of the same reservoir production phase. In particular, results from the precedent computation are compared with those ones obtained from the application of a non-coupled fracture model on the same reservoir schematization using the same initial and boundary conditions. From the comparisons appears that the fracture closure variation, described by the coupled model, heavily influences all the hydraulic parameters.

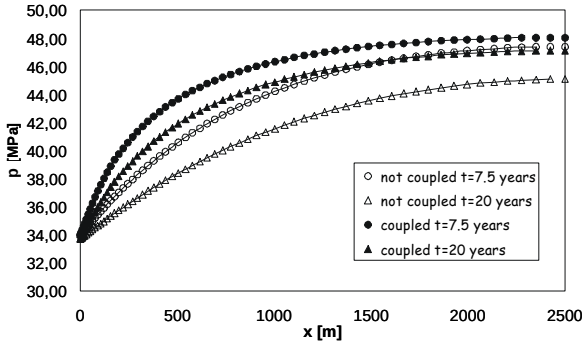

Figure 11. Fluid pressure – comparison between coupled and non-coupled fracture model.

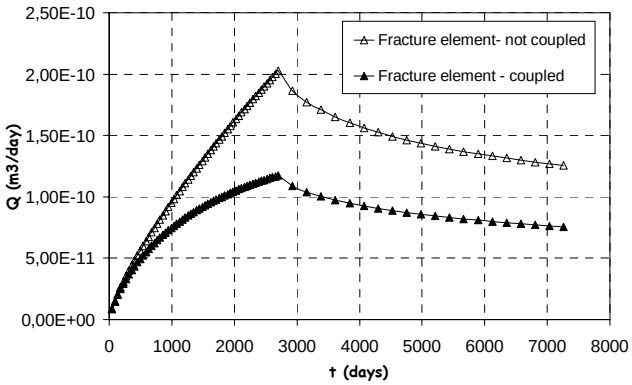

Figure 12. Flow rate trend comparison using a coupled and a non-coupled fracture model.

More in detail, comparisons with the non-coupled model show that the progressive fracture closure is responsible of: 1) a slower fluid pressure decrease along the fracture (Fig. 11) and a lower fluid flow value along all the fracture; 2) a smaller quantity of flow rate outgoing from the fracture to the well boundary (Fig. 12).

4.4 *Sensitivity study*

Two different sensitivity studies were performed in the following to test the correct description given by the presented coupled model. Both studies were performed starting from the same reservoir configuration of the previous simulations. Keeping the same initial conditions, different essays were developed applying different boundary hydraulic conditions. In the first study (Fig. 13) a fluid pressure depletion of 10 MPa was applied at different time intervals (6 months, 1, 7.5 and 15 years). In the second study three essays are developed using three different fluid pressure depletions respectively of 5, 10 and 20 MPa applied at the same time step of 7.5 years (Fig. 13). During both studies, after the respectively depletion phase, pressure is maintained constant until 20 years of simulation time.

Results about the first study show that the highest flow rate peak value is achieved for short time step (6 months) of 10 MPa depletion, while the lowest value is obtained for a Δp =10 MPa applied during a time step of 15 years. So, to faster applications of the fluid pressure variation at the well boundary, it's observed, in the flow rate curves, the presence of higher peaks reached in shorter times (Fig. 14). It's also observed that, at long terms, the different flow rate curves trends related to this study reach more or less the same value.

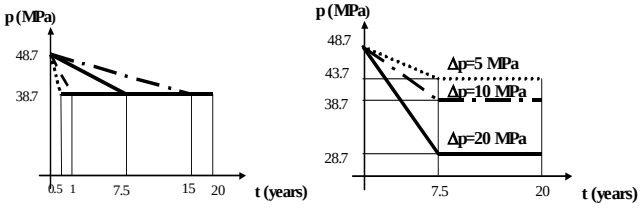

Figure 13. Hydraulic boundary condition for the first sensitivity case (Left) and the second one (Right).

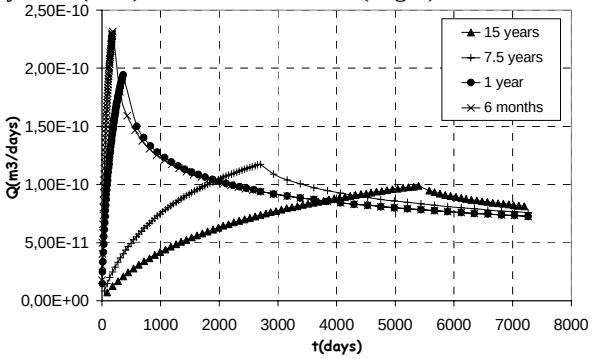

Figure 14. First sensitivity study results - Different flow rate path applying a 10 MPa depletion respectively in 6 months, 1, 7.5 and 15 years.

Further results on fracture opening illustrate, once more, the direct proportionality between the Δp application velocity and the closure fracture variation.

Second sensitivity study results show, this time, the existence of a non-proportional correspondence between both Δp applied steps with flow rate curves (Fig. 15) and Δp with fracture closure variation (Fig. 16).

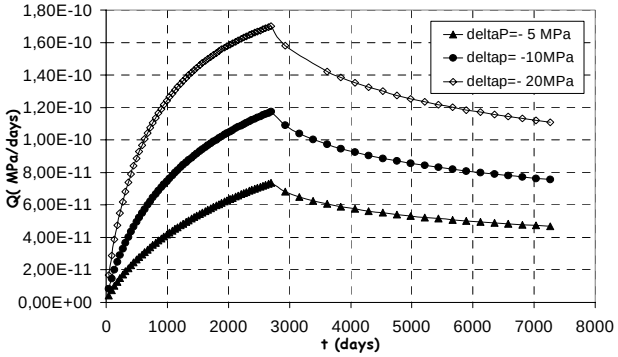

Figure 15. Second sensitivity study results - Different flow rate path for 5, 10 and 20 MPa imposed pressure variation.

5 CONCLUSIONS

A coupled fracture model was developed in this paper to predict the influence of the hydro-mechanical fracture behavior in the oil reservoir exploitation. It combines the cubic law with a non-linear deformation fiunction (hyperbolic) suggested to describe the stress-closure/opening curves of the joints.

Then the model was implemented in the finite element code LAGAMINE in order to be validated.

Academic simulations and comparisons using a non-coupled model were performed to show the two main advantages of the presented methodology. First one, the innovative description of the fracture behavior obtained by taking into account both the hydraulic and mechanical aspect. This is in contrast with the actual oil companies tendency to consider fractures influence on the reservoir only from an hydraulic point of view. Second one, the attempt to offer a representative description of fractured oil reservoirs through a finite element schematization where only the main fractures were reproduced. These tools avoid the difficulties for a numerical code to reproduce a complex and non-homogeneous fracture field.

Further applications to real fractured oil reservoir geometry will be developed in the future.

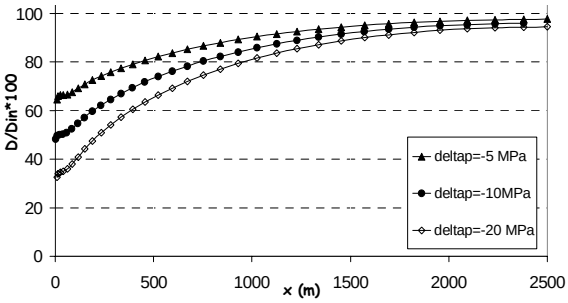

Figure 16. Second sensitivity study results - Closure fracture variation after 7.5 years.

REFERENCES

Bandis, S. Lumsden, A.C. & Barton, N. 1981. Experimental studies of scale effects on the shear behavior of rock joints. *Int. Jour. Of Rock Mechanics and mining Science & Geomech. Abstr.* Vol. 18(1), pp. 1-21.

Bandis, S. Lumsden, A.C. & Barton, N. 1983. Foundamentals of rock joints deformation. *Int. Jour. Of Rock Mechanics and mining Science & Geomech. Abstr.* Vol. 20(6), pp. 249-68.

Bart, M. 2000. Contribution à la modélisation du comportement hydromécanique des massifs rocheux avec fracture. *Ph. D. Thesis, Univ. des Sciences et Technologies de Lille.*

Barton, N. Choubey, V. 1976. The shear strenght of rock joints in theory and practice. *Rock Mechanics and Rock Engineering.* Vol. 10, pp. 1-54.

Barton, N. Bandis, S. & Bakhtar, K. 1985. Strenght deformation and conductivity coupling of rock joints. *Int. Jour. Of Rock Mechanics and mining Science & Geomech. Abstr.* Vol. 22(3), pp. 121-140.

Charlier, R. Cescotto, S. 1988. Modélisation du phénomène de contact unilatéral avec frottement dans un contexte de grandes déformations. *Jl. Of Theorical and Applied Mechanics (special issue, supplement)*, Vol. 7(1).

Cescotto, S. Charlier, R. 1993. Frictional contact finite elements based on mixed variational principles. *Int. Jl. For Numerical Methods in Engineering*, Vol. 36, pp. 1681-1701.

Goodman, R. Taylor, R. & Brekke, T. 1968. A model for the mechanics of jointed rock. *J. Soil Mech. Fdns Div., Proc. Am. Soc.civ. Engr*, N° 94, pp. 637-659.

Goodman, R. Debois, J. 1972. Duplication of dilatancy in analysis of jointed rocks. *Journal of the soil mechanics and foundations division, ASCE*, Vol. 98, SM 4 pp. 399-422.

Goodman, R. 1974. The mechanical properties of joints. *Proc. 3D Congr. ISRM*, Denver, Vol. 1a, pp. 127-140.

Habraken, A.M. Cescotto, S. 1996. Contact between deformable solids. The fully coupled approach. *Jl. For Mathematical and Computer Modelling (special issue: Recent advances in contact and impact mechanics).*

Plesha, M. E. 1995. Rock joints: Theory, constitutive equations. *Studies in applied mechanics 42, Mechanics of geomaterials interfaces*, ELSEVIER, pp. 375-394.

Tsang, Y. W. Witherspoon, P. A. 1981. Hydromechanical behavior of a deformable rock fracture subject to normal stress. *J. Geophys. Res.* 86, pp. 9287-9298.